

Spectroscopy at Belle II

Alessandro Boschetti^{a,b} on behalf of the Belle II collaboration

^a*University of Turin,
via Verdi 8, Turin, Italy*

^b*Istituto Nazionale di Fisica Nucleare - Sezione di Torino,
via Pietro Giuria 1, Turin, Italy*

E-mail: boschett@to.infn.it

The Belle II experiment offers unique possibilities for discovering and interpreting exotic multi-quark bound states to probe the fundamentals of QCD. We present recent results obtained on a unique data set collected at energies above the $Y(4S)$, including searches for the hidden bottom transition between $Y(10750)$ and $\chi_{bJ}(1P)$ and the measurement of the energy dependence of the $e^+e^- \rightarrow b\bar{b}$ cross section.

*Workshop Italiano sulla Fisica ad Alta Intensità (WIFAI 2023)
November 8, 2023 to November 10, 2023
Dipartimento di Architettura dell'Università Roma Tre*

1. Introduction

Quarkonium spectroscopy is an excellent probe for the study of QCD in the non-perturbative regime [1]. In recent years various collaborations, in particular experiments at e^+e^- colliders, discovered a number of unexpected quarkonium-like states labeled as X, Y, and Z states in both the charmonium and bottomonium mass regions. Since the properties of these exotic hadrons are not predicted by the quark model, different partonic arrangements are being considered, such as compact tetraquarks, mesonic molecules and hybrids [2]. More experimental results are needed in this sector for a better understanding of the phenomenology of quarkonium(-like) states and transitions.

The new asymmetric-energy e^+e^- collider SuperKEKB, located at the KEK research facility in Tsukuba, Japan, operates at center-of-mass energy close to the mass of the $\Upsilon(4S)$ resonance in order to study CP violation in the B sector. However, the beam energies can be tuned to perform energy scans that are needed for bottomonium spectroscopy studies. The SuperKEKB collider detains the world record peak instantaneous luminosity $\mathcal{L} = 4.7 \times 10^{34} \text{ cm}^{-2}\text{s}^{-1}$ [3] which has allowed Belle II to collect a data set corresponding to an integrated luminosity of 428 fb^{-1} in a few years of operation. The target instantaneous luminosity of $6 \times 10^{35} \text{ cm}^{-2}\text{s}^{-1}$ will enable Belle II to collect a projected integrated luminosity of 50 ab^{-1} over the next decade.

The Belle II detector is a general purpose, nearly 4π magnetic spectrometer incorporating state of the art technology for tracking, calorimetry and particle identification. It consists of several sub-detectors. Two layers of pixelated silicon detectors (PXD) and four layers of double-sided silicon strip sensor (SVD) measure the decay vertex position. The central drift chamber (CDC) allows to measure the trajectories, momenta and dE/dx of charged particles. The barrel-shaped Time-Of-Propagation (TOP) detector and the ring-imaging aerogel Cherenkov radiator (ARICH) measure the Cherenkov radiation for particle identification in the barrel and forward end-cap regions respectively. The K-Long and Muon (KLM) detector located outside of the superconducting coil is used to detect K_L^0 mesons and identify muons. The details of the Belle II detector are described elsewhere [4].

2. Observation of $e^+e^- \rightarrow \omega\chi_{bJ}(1P)$ and search for $X_b \rightarrow \omega\Upsilon(1S)$ at \sqrt{s} near 10.75 GeV

Recently, the Belle collaboration observed a new structure in e^+e^- collisions at center-of-mass energies between 10.52 and 11.02 GeV [6] decaying to $\Upsilon(nS)\pi^+\pi^-$ ($n = 1, 2, 3$), referred to as Y(10753). To confirm the existence of this new state and study its properties, Belle II performed an energy scan in the proximity of Y(10753), collecting data corresponding to an integrated luminosity of 19.3 fb^{-1} at the four center-of-mass energy points $\sqrt{s} = 10.653, 10.701, 10.745, 10.805 \text{ GeV}$.

The unknown nature of the Y(10753) state is generating a wide interest on the theoretical side. As the newly observed state does not correspond to any pure $b\bar{b}$ resonance, the most conventional interpretations describe Y(10753) as a mixture of the $\Upsilon(4S)$ and $\Upsilon(3D)$ states [7, 8]. Other interpretations consider the state as a hybrid [9] or tetraquark [11, 21] candidate. Models that describe the Y(10753) state as an admixture of the conventional $4S$ and $3D$ states predict

comparable branching fractions for the $Y(10753) \rightarrow \pi^+\pi^-Y(nS)$ and $Y(10753) \rightarrow \omega\chi_{bJ}(1P)$ decays [13]. Moreover, the ratio $\frac{\mathcal{B}[Y(10753) \rightarrow \omega\chi_{b1}(1P)]}{\mathcal{B}[Y(10753) \rightarrow \omega\chi_{b2}(1P)]}$ is expected to be about 1/5 [14].

We tested these predictions by measuring the $\sigma(e^+e^- \rightarrow \omega\chi_{bJ}(1P))$ cross section [15]. An analogous measurement was made at Belle at $\sqrt{s} = 10.867$ GeV [16]. The $\omega\chi_{bJ}(1P)$ final state is reconstructed exclusively through the $\omega \rightarrow \pi^+\pi^-\pi^0$ decay, the $\chi_{bJ}(1P)$ radiative transition to $\gamma Y(1S)$ final state and the $Y(1S) \rightarrow l^+l^-$ di-lepton decays, where $l = \mu, e$.

Pions are identified with 90% efficiency, and at least one of the leptons is identified with 95% efficiency for electrons and 90% efficiency for muons. To reduce the effects of bremsstrahlung and final-state radiation, photons within a 50 mrad cone from the electron or positron direction contribute to the calculation of the particle four-momentum. Photons used to reconstruct π^0 candidates are required to have energies greater than 25, 25, and 40 MeV, when detected in the barrel, forward end-cap, and backward end-cap respectively, and to satisfy $105 < M(\gamma\gamma) < 150$ MeV/ c^2 . The $Y(1S)$ signal regions are selected by requiring $9.25 < M(e^+e^-) < 9.58$ GeV/ c^2 and $9.34 < M(\mu^+\mu^-) < 9.58$ GeV/ c^2 . We apply a four-constraint (4C) kinematic fit that constrains the total four-momentum of the $\pi^+\pi^-\pi^0 Y(1S)$ combination to the beam four-momentum. In events where more than one candidate is found, we keep only the one with the lowest χ^2 .

The signal yields for the processes $e^+e^- \rightarrow \omega\chi_{bJ}(1P)$ are measured by performing a two-dimensional unbinned maximum likelihood fit to the joint distribution of $M(\pi^+\pi^-\pi^0)$ and $M(\gamma Y(1S))$. The measurement is done at the three energy points $\sqrt{s} = 10.701, 10.745, 10.805$ GeV. The measurements are combined with the results from Belle $\sigma_B(e^+e^- \rightarrow \omega\chi_{b1}) = (0.76 \pm 0.16)$ pb and $\sigma_B(e^+e^- \rightarrow \omega\chi_{b2}) = (0.29 \pm 0.14)$ pb at $\sqrt{s} = 10.867$ GeV [16], as shown in figure 1. We fit the energy dependence of the cross section with a coherent sum of a two-body phase space and a Breit-Wigner function. We observe a significant signal for $e^+e^- \rightarrow \omega\chi_{b1}(1P)$ and evidence for $e^+e^- \rightarrow \omega\chi_{b2}(1P)$. At $\sqrt{s} = 10.745$ GeV, we measure the ratio $\sigma(e^+e^- \rightarrow \omega\chi_{b1})/\sigma(e^+e^- \rightarrow \omega\chi_{b2}) = 1.3 \pm 0.6$, which is inconsistent with the prediction for a pure D -wave bottomonium state [19] and in 1.8σ tension with the prediction for a $S - D$ mixed state [14].

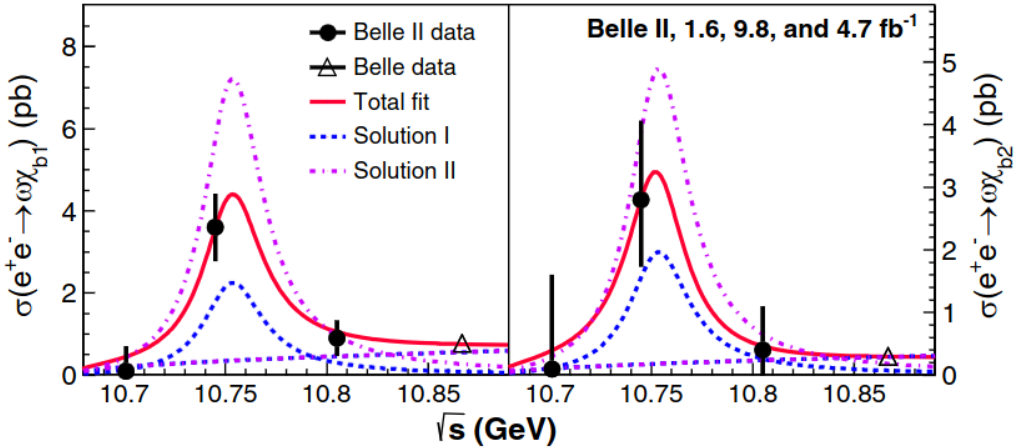


Figure 1: Energy dependence of the $e^+e^- \rightarrow \omega\chi_{b1}$ (left) and $e^+e^- \rightarrow \omega\chi_{b2}$ (right) cross sections. Circles are the results obtained with the Belle II data and triangles are the result of the Belle analysis. The error bars represent the combined statistical and systematic uncertainties. The red curve show the fit result and the dashed curves the components of the fit function.

In addition, the same final state is used to search for the bottomonium analog of the $X(3872)$ state, denoted as X_b , via the process $e^+e^- \rightarrow \gamma X_b \rightarrow \gamma \omega \Upsilon(1S)$. This is motivated by the observation of the analogous cascade decay in the charmonium sector $Y(4240) \rightarrow \gamma X(3872) \rightarrow \gamma \omega J/\psi$ by the BESIII collaboration [17]. Figure 2 shows the reconstructed $\omega \Upsilon(1S)$ invariant mass distribution. While a reflection of the $e^+e^- \rightarrow \omega \chi_{bJ}$ signal is observed, no narrow structure consistent with the X_b signal is visible. We set upper limits at 90% Bayesian credibility on the product of the Born cross section $\sigma(e^+e^- \rightarrow \gamma X_b)$ and of the branching ratio $\mathcal{B}[X_b \rightarrow \omega \Upsilon(1S)]$. The results at all center-of-mass energies are reported in table 1.

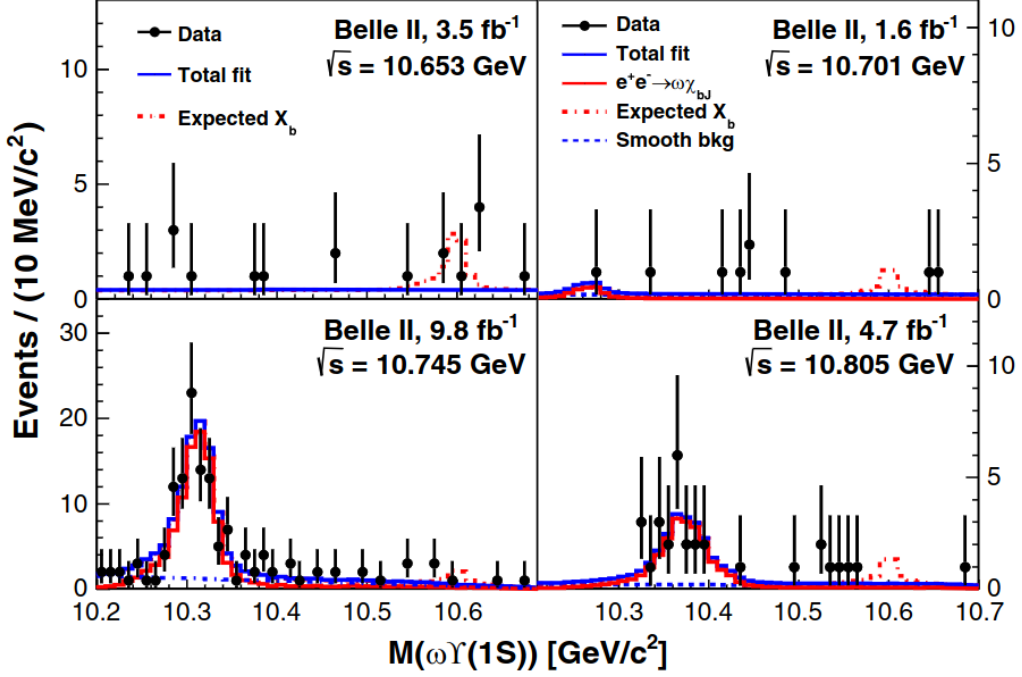


Figure 2: Distributions of the $\omega \Upsilon(1S)$ invariant mass at $\sqrt{s} = 10.653, 10.701, 10.745,$ and 10.805 GeV. The red dash-dotted histograms correspond to the expected X_b signal with mass $10.6 \text{ GeV}/c^2$ with yields corresponding to the upper limit values.

Table 1: Upper limits at 90% Bayesian credibility level at different center-of-mass energies for $\sigma_{X_b}^{UL} = \sigma(e^+e^- \rightarrow \gamma X_b) \times \mathcal{B}[X_b \rightarrow \omega \Upsilon(1S)]$.

\sqrt{s} (GeV)	M_{X_b} (GeV/ c^2)	$\sigma_{X_b}^{UL}$ (pb)
10.653	10.59	0.55
10.701	10.45	0.84
10.745	10.45	0.14
10.805	10.53	0.47

3. Search for $e^+e^- \rightarrow \chi_{b0}(1P)\omega, \eta_b(1S)\omega$

We report the search for the two transitions to hidden bottom states with the emission of an ω meson $e^+e^- \rightarrow \chi_{b0}(1P)\omega, \eta_b(1S)\omega$ at $\sqrt{s} = 10.745$ GeV. A recent model that interprets the $Y(10753)$ state as a tetraquark [21] predicts a strong enhancement of the cross section for the $\eta_b(1S)\omega$ final state with respect to $Y(10753) \rightarrow Y(nS)\pi^+\pi^-$. The analysis is further motivated by the recent observation of the $Y(4220) \rightarrow \chi_{c0}(1P)\omega$ decay [12], which is enhanced with respect to the $Y(4220) \rightarrow \chi_{c1,2}(1P)\omega$ modes. Since the $\chi_{b0}(1P)$ and $\eta_b(1S)$ states do not have exclusive decays with high branching ratio, this analysis is fully inclusive. Only the $\omega \rightarrow \pi^+\pi^-\pi^0$ decay is reconstructed, and the signals are searched for by looking at the recoil mass $M_{recoil}(\pi^+\pi^-\pi^0) = \sqrt{(E_{c.m.} - E^*)^2 - (p^*)^2}$, where $E_{c.m.}$ is the center of mass energy of the initial state, and E^* and p^* are respectively the energy and momentum of the ω in the center of mass frame.

The reconstructed ω mass is required to be within ± 13 MeV/ c^2 the PGD value. We perform a least-squares fit to the $M_{recoil}(\pi^+\pi^-\pi^0)$ distribution. The signal shape is modeled by a sum of a Gaussian function and a double-sided Crystal Ball (CB) function, while the background is described by second and third order polynomials for the $\eta_b(1S)\omega$ and $\chi_{b0}(1P)\omega$ channels, respectively. The orders of the polynomial functions are chosen to give the maximal p -value for the fit. The fit intervals are (9.200, 9.600) GeV/ c^2 and (9.780, 9.950) GeV/ c^2 for the $\eta_b(1S)$ and $\chi_{b0}(1P)$ candidates, respectively.

No signal is observed, thus we set 90% CL upper limits $\sigma(e^+e^- \rightarrow \chi_{b0}(1P)\omega) < 8.7$ pb, $\sigma(e^+e^- \rightarrow \eta_b(1S)\omega) < 2.5$ pb. These results exclude the tetraquark model in [21].

4. Energy dependence of the $e^+e^- \rightarrow B\bar{B}, B\bar{B}^*, B^*\bar{B}^*$ cross sections

The cross section of the e^+e^- annihilation into hadrons is often reported by means of the R ratio

$$R = \frac{\sigma(e^+e^- \rightarrow \text{hadrons})}{\sigma^B(e^+e^- \rightarrow \mu^+\mu^-)} \quad (1)$$

where $\sigma^B(e^+e^- \rightarrow \mu^+\mu^-)$ is the Born cross section for $e^+e^- \rightarrow \mu^+\mu^-$. While many precise measurements of R at low energies are available, those at higher energies, such as the bottomonium region, are sparser and less precise. This is mainly due to the fact that the $b\bar{b}$ region has been accessible to fewer experiments. The BaBar and Belle collaborations measured the cross section of $e^+e^- \rightarrow b\bar{b}$ at center-of-mass energies ranging from 10.5 to 11.2 GeV [20, 22] by defining the ratio

$$R_b = \frac{\sigma(e^+e^- \rightarrow b\bar{b})}{\sigma^B(e^+e^- \rightarrow \mu^+\mu^-)}. \quad (2)$$

Belle II has the capability to improve the measurement of R_b by including new energy points. The predominant decay modes of bottomonium states above $B\bar{B}$ threshold are expected to be the open flavor channels $B\bar{B}, B\bar{B}^*, B^*\bar{B}^*$. The sum of the corresponding cross sections is expected to saturate the $e^+e^- \rightarrow b\bar{b}$ cross section. Thus, the measurement of the exclusive $e^+e^- \rightarrow B^{(*)}\bar{B}^{(*)}$ cross sections provides important information on the interactions in this energy region and in particular about the structure of bottomonium(-like) resonances. This topic is of special interest since all the states above threshold exhibit anomalies, especially in transitions to lower bottomonia,

which currently are not well understood [23]. The analysis follows the analogous measurement performed at Belle [26].

The method we follow consists in fully reconstructing one B meson in hadronic decay modes using the Full Event Interpretation (FEI) algorithm [25], and identifying the $B\bar{B}$, $B\bar{B}^*$, and $B^*\bar{B}^*$ signals in the distribution of the beam-constrained mass $M_{bc} = \sqrt{(E_{c.m.}/2)^2 - p_B^2}$, where p_B is the momentum of the reconstructed B candidate. For $B\bar{B}$ pairs, the M_{bc} distribution peaks at the nominal B mass m_B , while for $B\bar{B}^*$ and $B^*\bar{B}^*$ pairs it peaks approximately at $m_B + \frac{\Delta m_{B^*}}{2}$ and $m_B + \Delta m_{B^*}$ respectively, where Δm_{B^*} is the mass difference between the B^* and B mesons. The M_{bc} distribution obtained at $\sqrt{s} = 10.746$ GeV is shown in figure 3a. All the four scan points at $\sqrt{s} = 10.653, 10.701, 10.745, 10.805$ GeV are used in this analysis.

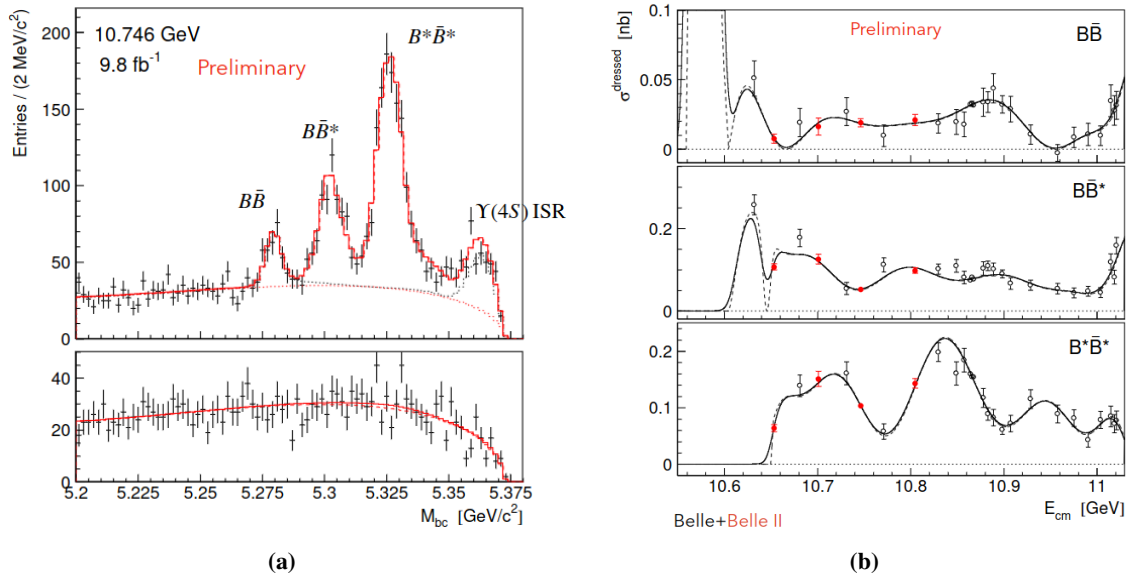


Figure 3: Preliminary results of the measurement of the $e^+e^- \rightarrow B\bar{B}, B\bar{B}^*, B^*\bar{B}^*$ cross sections using the Belle II scan data. The signal yields are obtained by fitting the M_{bc} distributions (a) at each value of \sqrt{s} . Figure (b) shows the energy dependence of the Born cross section, combined with the measurement from Belle. The red (black) points correspond to the Belle II (Belle) measurement.

The signal yields are estimated by fitting the M_{bc} distributions. The fit function for the signal and peaking background components is constructed in the same way as in ref. [26]. We measure the dressed cross section, which accounts for the vacuum polarization. From the yield N of a specific decay mode, the corresponding dressed cross section is calculated as

$$\sigma^{\text{dressed}} = \frac{N}{(1 + \delta_{ISR})L\varepsilon} \quad (3)$$

where $(1 + \delta_{ISR})$ is the radiative correction factor, L is the integrated luminosity and ε is the reconstruction efficiency. We fit simultaneously the energy dependence of the $e^+e^- \rightarrow B\bar{B}, B\bar{B}^*, B^*\bar{B}^*$ cross sections and of the total $e^+e^- \rightarrow b\bar{b}$ cross section. The results are shown in Fig. 3b, where the previous measurement from Belle is included.

5. Summary

We have shown recent measurements performed by the Belle II collaboration using the data set collected in an energy scan above the $Y(4S)$ resonance. We observe significant signals for the $Y(10753) \rightarrow \omega \chi_{bJ}(1P)$, $J = 1, 2$ decays. Moreover, from the ratio of the two corresponding cross sections, we exclude a conventional $b\bar{b}$ interpretation for the $Y(10753)$ state [19]. No significant signal is observed for the production of the X_b state, the analogue of $X(3872)$ in the bottomonium sector, in $e^+e^- \rightarrow \gamma X_b \rightarrow \gamma \omega Y(1S)$. We set 90% CL upper limits for the $Y(10753) \rightarrow \omega \chi_{b0}(1P)$ and $Y(10753) \rightarrow \omega \eta_b(1S)$ decays, which exclude the compact tetraquark interpretation described in Ref. [21]. Finally, we report the measurement of the energy dependence of the $e^+e^- \rightarrow B\bar{B}$, $B\bar{B}^*$, $B^*\bar{B}^*$ cross sections. This measurement is combined with the previous Belle result [26], allowing to improve the fit to the experimental data.

These results are of great importance in understanding the nature of the new $Y(10753)$ state and, more generally, of the bottomonium(-like) states above the open flavor threshold. The uniqueness of the data set collected at center-of-mass energies around 10.75 GeV will enable Belle II to provide unprecedented results in the quarkonium sector in the near future.

References

- [1] N. Brambilla *et al.* [Quarkonium Working Group], doi:10.5170/CERN-2005-005 [arXiv:hep-ph/0412158 [hep-ph]].
- [2] N. Brambilla, S. Eidelman, C. Hanhart, A. Nefediev, C. P. Shen, C. E. Thomas, A. Vairo and C. Z. Yuan, Phys. Rept. **873** (2020), 1-154 doi:10.1016/j.physrep.2020.05.001 [arXiv:1907.07583 [hep-ex]].
- [3] T. Abe, K. Akai, N. Akasaka, M. Akemoto, A. Akiyama, M. Arinaga, Y. Cai, K. Ebihara, K. Egawa and A. Enomoto, *et al.* PTEP **2013** (2013), 03A001 doi:10.1093/ptep/pts102
- [4] T. Abe *et al.* [Belle-II], [arXiv:1011.0352 [physics.ins-det]].
- [5] T. Kuhr *et al.* [Belle-II Framework Software Group], Comput. Softw. Big Sci. **3** (2019) no.1, 1 doi:10.1007/s41781-018-0017-9 [arXiv:1809.04299 [physics.comp-ph]].
- [6] R. Mizuk *et al.* [Belle], JHEP **10** (2019), 220 doi:10.1007/JHEP10(2019)220 [arXiv:1905.05521 [hep-ex]].
- [7] B. Chen, A. Zhang and J. He, Phys. Rev. D **101** (2020) no.1, 014020 doi:10.1103/PhysRevD.101.014020 [arXiv:1910.06065 [hep-ph]].
- [8] J. F. Giron and R. F. Lebed, Phys. Rev. D **102** (2020) no.1, 014036 doi:10.1103/PhysRevD.102.014036 [arXiv:2005.07100 [hep-ph]].
- [9] P. Bicudo, N. Cardoso, L. Mueller and M. Wagner, Phys. Rev. D **103** (2021) no.7, 074507 doi:10.1103/PhysRevD.103.074507 [arXiv:2008.05605 [hep-lat]].

- [10] Z. G. Wang, Chin. Phys. C **43** (2019) no.12, 123102 doi:10.1088/1674-1137/43/12/123102 [arXiv:1905.06610 [hep-ph]].
- [11] A. Ali, L. Maiani, A. Y. Parkhomenko and W. Wang, Phys. Lett. B **802** (2020), 135217 doi:10.1016/j.physletb.2020.135217 [arXiv:1910.07671 [hep-ph]].
- [12] M. Ablikim *et al.* [BESIII], Phys. Rev. D **99** (2019) no.9, 091103 doi:10.1103/PhysRevD.99.091103 [arXiv:1903.02359 [hep-ex]].
- [13] Z. Y. Bai, Y. S. Li, Q. Huang, X. Liu and T. Matsuki, Phys. Rev. D **105** (2022) no.7, 074007 doi:10.1103/PhysRevD.105.074007 [arXiv:2201.12715 [hep-ph]].
- [14] Y. S. Li, Z. Y. Bai, Q. Huang and X. Liu, Phys. Rev. D **104** (2021) no.3, 034036 doi:10.1103/PhysRevD.104.034036 [arXiv:2106.14123 [hep-ph]].
- [15] I. Adachi *et al.* [Belle-II], Phys. Rev. Lett. **130** (2023) no.9, 091902 doi:10.1103/PhysRevLett.130.091902 [arXiv:2208.13189 [hep-ex]].
- [16] X. H. He *et al.* [Belle], Phys. Rev. Lett. **113** (2014) no.14, 142001 doi:10.1103/PhysRevLett.113.142001 [arXiv:1408.0504 [hep-ex]].
- [17] M. Ablikim *et al.* [BESIII], Phys. Rev. Lett. **122** (2019) no.23, 232002 doi:10.1103/PhysRevLett.122.232002 [arXiv:1903.04695 [hep-ex]].
- [18] Y. Iwasaki, B. Cheon, E. Won, X. Gao, L. Macchiarulo, K. Nishimura and G. Varner, IEEE Trans. Nucl. Sci. **58** (2011), 1807-1815 doi:10.1109/TNS.2011.2119329
- [19] F. K. Guo, U. G. Meißner and C. P. Shen, Phys. Lett. B **738** (2014), 172-177 doi:10.1016/j.physletb.2014.09.043 [arXiv:1406.6543 [hep-ph]].
- [20] B. Aubert *et al.* [BaBar], Phys. Rev. Lett. **102** (2009), 012001 doi:10.1103/PhysRevLett.102.012001 [arXiv:0809.4120 [hep-ex]].
- [21] Z. G. Wang, Chin. Phys. C **43** (2019) no.12, 123102 doi:10.1088/1674-1137/43/12/123102 [arXiv:1905.06610 [hep-ph]].
- [22] D. Santel *et al.* [Belle], Phys. Rev. D **93** (2016) no.1, 011101 doi:10.1103/PhysRevD.93.011101 [arXiv:1501.01137 [hep-ex]].
- [23] A. E. Bondar, R. V. Mizuk and M. B. Voloshin, Mod. Phys. Lett. A **32** (2017) no.04, 1750025 doi:10.1142/S0217732317500250 [arXiv:1610.01102 [hep-ph]].
- [24] R. Mizuk *et al.* [Belle], JHEP **06** (2021), 137 doi:10.1007/JHEP06(2021)137 [arXiv:2104.08371 [hep-ex]].
- [25] T. Keck, F. Abudinén, F. U. Bernlochner, R. Cheaib, S. Cunliffe, M. Feindt, T. Ferber, M. Gelb, J. Gemmler and P. Goldenzweig, *et al.* Comput. Softw. Big Sci. **3** (2019) no.1, 6 doi:10.1007/s41781-019-0021-8 [arXiv:1807.08680 [hep-ex]].
- [26] R. Mizuk *et al.* [Belle], JHEP **06** (2021), 137 doi:10.1007/JHEP06(2021)137 [arXiv:2104.08371 [hep-ex]].